Electronic Materials Letters, Vol. 8, No. 6 (2012), pp. 639-642
DOI: 10.1007/s13391-012-2029-7

Comparison of Nanostructured Nickel Zinc Ferrite and Magnesium Copper Zinc Ferrite Prepared by Water-In-Oil Microemulsion

Ay Ching Hee,[1] Mehdi Mehrali,[1,*] Hendrik Simon Cornelis Metselaar,[1] Mohammad Mehrali,[1] and Noor Azuan Abu Osman[2]

[1]Center of Advanced Materials, Department of Mechanical Engineering, Faculty of Engineering, University of Malaya, 50603 Kuala Lumpur, Malaysia
[2]Department of Biomedical Engineering, Faculty of Engineering, University of Malaya, 50603 Kuala Lumpur, Malaysia

(received date: 5 March 2012 / accepted date: 5 July 2012 / published date: December 2012)

Ferrite is an important ceramic material with magnetic properties that are useful in many types of electronic devices. In this study, structure and magnetic properties of nanostructured nickel zinc ferrite and magnesium copper zinc ferrite prepared by water-in-oil microemulsion were compared. Both ferrites samples demonstrated similar weight loss characteristics in TGA. The magnesium copper zinc ferrite showed a crystalline structure with an average crystallite size of 13.5 nm. However, nickel zinc ferrite showed an amorphous phase. Transmission electron micrographs showed agglomerated nanoparticles with an average crystallite size of 26.6 nm for magnesium copper zinc ferrite and 22.7 nm for nickel zinc ferrite. Magnesium copper zinc ferrite exhibited soft ferromagnetic bahaviour whereas nickel zinc ferrite showed superparamagnetic nature.

Keywords: ferrite, chemical synthesis, magnetic measurements, microstructure

1. INTRODUCTION

Ferrites are important chemical compounds used in information storage systems, magneto-caloric refrigeration, ferrofluid technology, and medical diagnosis due to its chemical stability and high magnetocrystalline anisotropy.[1] Magnesium copper zinc ferrite and nickel zinc ferrite can be applied at a slew of frequencies ranging from 1 MHz to over 200 MHz and have great potential in the design of high-frequency devices such as micro-inductors and micro-transformers.[2] Magnesium copper zinc ferrites with low magnesium oxide (<10 mol. %), moderate copper oxide (10 - 20 mol. %) and high zinc oxide (>25 mol. %) contents have good electromagnetic properties.[3] It can be sintered at low temperature.[4-6] There are several techniques to produce ferrite powder. The most common method of preparing ferrite powder is the conventional solid-solution method, which nevertheless has some serious limitations.[7] Among the limitations, this method requires prolonged heating at high temperatures during their preparation, which may result in evaporation of some of the constituents, thereby changing the desired stoichiometry. Aggregation and coarsening of particles occur in the conventional solid-solution method.

Water-in-oil microemulsion is a promising preparation method for the formation of very fine and uniform nanoparticles with high chemical homogeneity.[8-10] The synthesis process is economical and environmentally friendly because it involves inexpensive and less toxic iron salts and a reduced amount of organic solvent.[11] In this study, nickel zinc ferrite and magnesium copper zinc ferrite were prepared by water-in-oil microemulsion. The structure and properties of the synthesized ferrites were compared using thermogravimetry, x-ray diffractometer, transmission electron microscope and alternating gradient magnetometer.

2. EXPERIMENTAL PROCEDURE

A reverse micelle solution was prepared by combining 0.56 M of sodium dioctylsulfosuccinate (AOT) (R&M Chemicals, UK) with a 2, 2, 4-trimethylpentane (isooctane) (Merck kGaA) oil phase. The reverse micelle solution was then divided into two halves. 0.07 M $FeCl_2.4H_2O$ (Strem Chemicals, USA), 0.02 M $NiCl_2.6H_2O$ (R&M Chemicals, UK), and 0.02 M $ZnCl_2$ (R&M Chemicals, UK) were mixed to make an aqueous solution containing the required metal ions. The water to surfactant ratio (w) was fixed at 15.5 and the relative volume of AOT solution to water as 6:1. The

*Corresponding author: m.mehrali@siswa.um.edu.my

first half of the reverse micelle solution was added volumetrically to the aqueous metal solution. An analogous solution that had been made using water and concentrated ammonia in a 1:1 ratio was added to the second half of the reverse micelle solution. Both the reverse micelle solutions containing metal aqueous solution and ammonia solution were agitated until each was visibly clear and transparent. The reverse micelle solution containing metal ions was placed in an addition funnel and added to the reverse micelle containing ammonia solution under constant stirring, allowing the reacting species to come in contact with each other due to the dynamic nature of the dispersed droplets. A green colour was formed immediately, after which the solution turned yellowish over a period of a few minutes. The mixture was stirred vigorously for two hours to complete the reaction. Excess methanol was added to the resulting mixture to disrupt the micelles and absorb surfactant molecules from the particles. The solution separated into two layers immediately after adding methanol showing an oily phase in the upper layer and a colourless phase for bottom part of the solution. The resulting product was collected by a centrifuge and washed repeatedly with methanol until all AOT was removed. The colloidal precipitate was then dried in a vacuum chamber for a 24 h.

The steps above were repeated to produce magnesium copper zinc ferrite with the same water to surfactant ratio (w) at 15.5. The only difference was that reverse micelle solution was prepared with 0.07 M $FeCl_2.4H_2O$ (Strem Chemicals, USA), 0.01 M $MgCl_2.6H_2O$ (Ajax Finechem, Australia), 0.03 M $CuCl_2.2H_2O$ (Fisher Chemicals, Malaysia) and 0.02 M $ZnCl_2$ (R&M Chemicals, UK) as the aqueous phase. Mettler TGA/SDTA851e Thermogravimetry Analysis (TGA) was performed to determine the calcination temperature of the ferrite samples. Structural characterization of the ferrites was carried out using Philips PW 3040 x-ray Diffractometer (XRD) and LEO-Libra 120 Transmission Electron Microscope (TEM). Magnetic property of the ferrites was characterized by MicroMag™ 2900 Alternating Gradient Magnetometer (AGM) from the Princeton Measurement Corporation.

3. RESULTS AND DISCUSSION

3.1 Thermogravimetric Analysis (TGA)

Thermogravimetric Analysis (TGA) was performed to determine the calcination temperature of the ferrite samples. Figure 1 shows the thermograms of $(Ni,Zn)Fe_2O_4$ (nickel zinc ferrite) and $(Mg,Cu,Zn)Fe_2O_4$ (magnesium copper zinc ferrite), where both samples have similar weight loss characteristics. The weight loss for both samples began from room temperature to 250°C, which is attributed to the dehydration of hydroxide complexes. The second degradation process occurred at around 600°C to 800°C and 850°C to 1000°C for

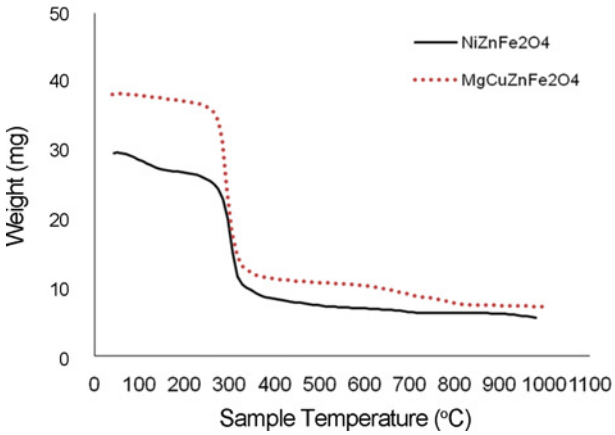

Fig. 1. Thermograms of nickel zinc ferrite and magnesium copper zinc ferrite.

$MgCuZnFe_2O_4$ and $NiZnFe_2O_4$, respectively. It indicates the ferritization process – a process where formation of ferrite takes place. As a result, $(Mg,Cu,Zn)Fe_2O_4$ and $(Ni,Zn)Fe_2O_4$ were calcined at 700°C and 900°C respectively for one hour with a heating rate of 4°C/min to ensure the complete dehydration and decomposition of the hydroxide complexes to form ferrite. The heating rate and duration of calcination were chosen to ensure homogeneous heating within the samples and also to prevent excessive self-heating which would lead to lack of chemical homogeneity and agglomeration.

3.2 X-ray Diffraction (XRD)

Figure 2 shows the XRD patterns of calcined magnesium copper zinc ferrite and nickel zinc ferrite nanoparticles. Magnesium copper zinc ferrite is polycrystalline as seen from the well-defined peaks in the pattern. All the basic components of $(Mg,Cu,Zn)Fe_2O_4$ powder in various oxidation states were detected in accordance with PDF#51-0384 from the International Centre for Diffraction Data (ICDD).

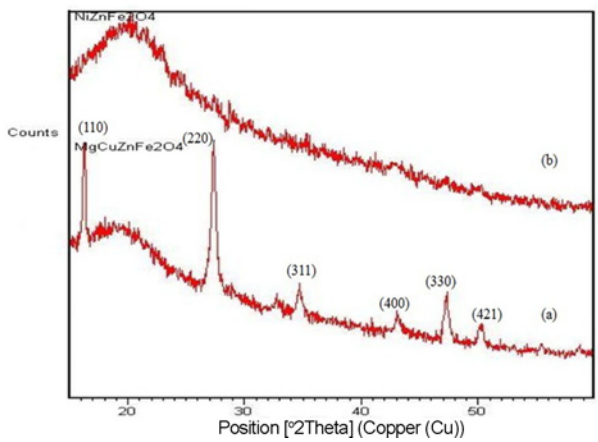

Fig. 2. X-ray diffraction patterns of (a) magnesium copper zinc ferrite and (b) nickel zinc ferrite nanoparticles.

The crystallite size was calculated using Scherrer's equation[12] from the broadened peak at $2\theta = 27.5°$, resulting in an average crystallite size of approximately 13.5 nm. A number of studies have been reported on the synthesis of nickel zinc ferrite using AOT and isooctane.[13,14] It was found that crystalline spinel ferrites were obtained even at lower calcination temperatures.

In this study, the XRD pattern of nickel zinc ferrite is amorphous. This is due to incomplete conversion of the hydroxide into the magnetic ferrite. A higher calcination temperature is suggested in order to obtain spinel nickel zinc ferrite.

3.3 Transmission Electron Microscope (TEM)

Figure 3 presents the transmission electron micrographs showing the morphologies of the ferrite nanoparticles. TEM studies in atomic resolution and electron diffraction have revealed that the synthesized $(Mg,Cu,Zn)Fe_2O_4$ nanoparticles have irregular shape and $(Ni,Zn)Fe_2O_4$ nanoparticles are roughly spherical in shape. $(Mg,Cu,Zn)Fe_2O_4$ is well dispersed, while $(Ni,Zn)Fe_2O_4$ shows severe aggregation.

This is thought to be due to the amorphous not using of the $(Ni,Zn)Fe_2O_4$.

In Fig. 4, $(Ni,Zn)Fe_2O_4$ nanoparticles have a more uniform size distribution compared to $(Mg,Cu,Zn)Fe_2O_4$ nanoparticles. The average size of $(Mg,Cu,Zn)Fe_2O_4$ and $NiZnFe_2O_4$ nanoparticles is 26.6 nm and 22.7 nm respectively, and this was calculated by measuring the diameters of 100 particles. The concentration of the reactants in the aqueous solution of reverse micelles influences the size of the product particles.[15] The particle size of magnesium copper zinc ferrite is slightly higher than that of nickel zinc ferrite due to the higher reactant concentration in magnesium copper zinc ferrite. The size of spherical nanoparticles is controlled by employing a low water to surfactant ratio (W = [water]/[surfactant]).[16-18] In other words, lower water contents were used in the synthesis process of nickel zinc ferrite particle and consequently resulting in a smaller particle size.

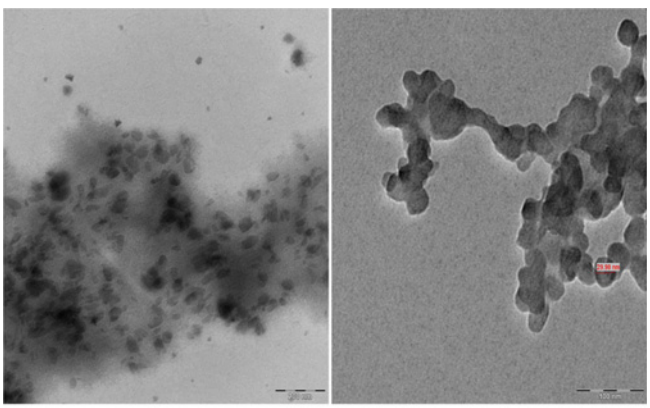

Fig. 3. Transmission electron micrographs show the microstructures of the (a) magnesium copper zinc ferrite and (b) nickel zinc ferrite nanoparticles.

3.4 Alternating Gradient Magnetometer (AGM)

Figure 5 presents the magnetic hysteresis curves of the calcined (a) $(Mg,Cu,Zn)Fe_2O_4$ and (b) $(Ni,Zn)Fe_2O_4$ nanoparticles. The M-H (magnetization versus magnetic field strength) curve of magnesium copper zinc ferrite displays ferromagnetic feature with a small hysteresis loop and coercivity value of 126 Oe. The M-H curve of nickel zinc ferrite indicates the presence of superparamagnetic nature with no hyteresis, remanence or coercivity. The saturation magnetization values for $(Mg,Cu,Zn)Fe_2O_4$ and $NiZnFe_2O_4$ are 28.66 emu/g and 16.10 emu/g respectively. The higher magnetization value of magnesium copper zinc ferrite was attributed to the high phase purity and well-defined crystallinity of its phase. Magnetization value at room temperature decreases sharply with decreasing crystalline size, which was first pointed out by Berkowitz and co-workers in the late sixties.[19] The smaller size range of nickel zinc ferrite caused the magnetization value to be lower.

Misra *et al.*[20] had reported that nanocrystalline ferrites

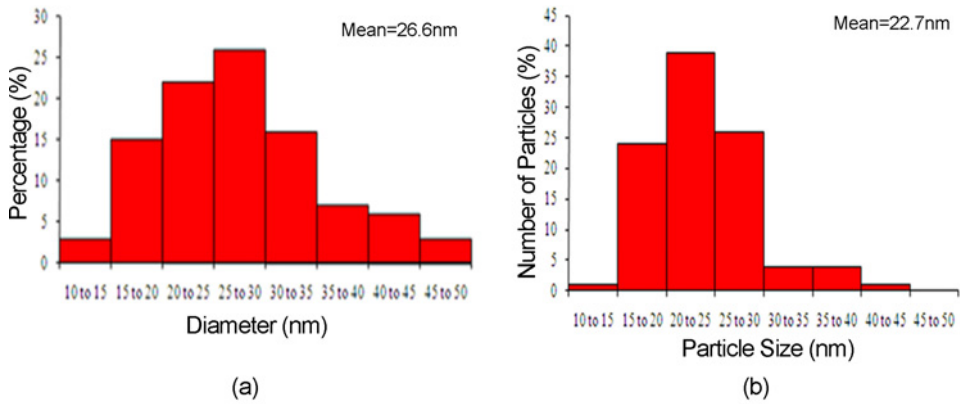

Fig. 4. Histogram of the particle size distribution obtained from (a) magnesium copper zinc ferrite and (b) nickel zinc ferrite nanoparticles.

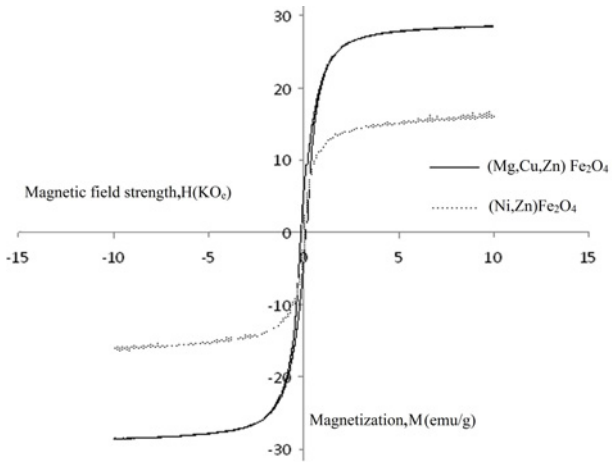

Fig. 5. Magnetization curves of calcined (a) magnesium copper zinc ferrite and (b) nickel zinc ferrite nanoparticles.

synthesized by the reverse micelle synthesis technique exhibit characteristics of superparamagnetism. In this case, magnesium copper zinc ferrite exhibited better magnetic property comparing with nickel zinc ferrite synthesized by water-in-oil microemulsion because of the ferromagnetic feature. According to Yang *et al.*[21 22], the transition of ferromagnetic to superparamagnetic in Co/Mo or Fe/Tb multilayer films were due to the structure transforms from bcc crystalline to amorphous. The magnetic properties of the synthesized ferrites were greatly influenced by the structure of its phase formed.

4. CONCLUSIONS

This work describes the comparison of nanostructured nickel zinc ferrite and magnesium copper zinc ferrite prepared by water-in-oil microemulsion technique, using dioctylsulfosuccinate as surfactant and ammonia as precipitant. Crystalline magnesium copper zinc ferrite nanoparticles were easily obtained by calcinating the ferrite sample at 700°C. However, The XRD pattern for nickel zinc ferrite nanoparticles was amorphous after calcination at 900°C. Magnesium copper zinc ferrite exhibited soft ferromagnetic bahaviour with a higher magnetization value. This is due to the high phase purity and well-defined crystallinity of its phase. The characteristics of soft ferromagnetism, that is, small hysteresis loss and low magnetic coercivity have been observed at room temperature. Magnesium copper zinc ferrite prepared by water-in-oil microemulsion has potential as magnetic building blocks in the development of multi-layer chip inductors as the coercivity value falls in the range of ferromagnetism. Magnetic bahavior of the synthesized ferrites depended very heavily on the structure and phase of the ferrites formed. The implication of ferrites structure in magnetic properties requires further investigation.

ACKNOWLEDGMENTS

The financial support received from Science Fund (03-01-03-SF0515), Ministry of Science, Technology and Innovation Malaysia and Ministry of Higher Education (MOHE) of Malaysia, grant number UM.C/HIR/MOHE/ENG/10 D000010-16001, University of Malaya is gratefully acknowledged.

REFERENCES

1. S. Kumar, V. Singh, S. Aggarwal, U. K. Mandal, and R. K. Kotnala, *Mater. Sci. Eng. B-Adv. Funct. Solid-State Mater.* **166**, 76 (2010).
2. S. Hashi, S. Yabukami, A. Maeda, N. Takada, S. Yanase, and Y. Okazaki, *J. Magn. Magn. Mater.* **316**, 465 (2007).
3. K. M. Hyie, I. Metselaar, and I. D. Yaacob, *Key Engineering Materials.* **306-308**, 875 (2006).
4. S. Murthy, *Bull. Mat. Sci.* **24**, 379 (2001).
5. N. Rezlescu, E. Rezlescu, P. D. Popa, M. L. Craus, and L. Rezlescu, *J. Magn. Magn. Mater.* **182**, 199 (1998).
6. Z. Yue, J. Zhou, L. Li, X. Wang, and Z. Gui, *Mater. Sci. Eng. B-Adv. Funct. Solid-State Mater.* **86**, 64 (2001).
7. R. G. Gupta and R. G. Mendiratta, *J. Appl. Phys.* **48**, 845 (1977).
8. A. B. Chin and I. I. Yaacob, *J. Mater. Process. Technol.* **191**, 235 (2007).
9. K. M. Hyie and I. I. Yaacob, *J. Mater. Process. Technol.***191**, 48 (2007).
10. Y. He, B. Yang, G. Cheng, and H. Pan, *Mater. Lett.* **58**, 2019 (2004).
11. D. S. Mathew and R. S. Juang, *Chem. Eng. J.* **129**, 51 (2007).
12. M. A. Gabal and Y. M. A. Angari, *Mater. Chem. Phys.* **118**, 153 (2009).
13. S. A. Morrison, C. L. Cahill, E. E. Carpenter, S. Calvin, R. Swaminathan, M. E. McHenry, and V. G. Harris, *J. Appl. Phys.* **95**, 6392 (2004).
14. S. Thakur, S. C. Katyal, and M. Singh, *J. Magn. Magn. Mater.* **321**, 1 (2009).
15. E. Anders and C. Palmqvist, *Curr. Opin. Colloid Interface Sci.* **8**, 145 (2003).
16. A. Caragheorgheopol, H. Caldararu, M. Vasilescu, A. Khan, D. Angelescu, N. Zilkova, and J. Cejka, *J. Phys. Chem. B.* **108**, 7735 (2004).
17. M. P. Pileni, *Nat Mater.* **2**, 145 (2003).
18. I. Capek, *Adv. Colloid Interface Sci.* **110**, 49 (2004).
19. A. E. Berkowitz, W. J. Schuele, and P. J. Flanders, *J. Appl. Phys.* **39**, 1261 (1968).
20. R. D. K. Misra, S. Gubbala, A. Kale, and W. F. Egelhoff Jr, *Mater. Sci. Eng. B-Adv. Funct. Solid-State Mater.* **111**, 167 (2004).
21. G. H. Yang, Y. Gu, Y. Gao, and F. Pan, *Thin Solid Films.* **457**, 354 (2004).
22. F. Yang, T. He, J. B. Chen, and F. Pan, *J. Appl. Phys.* **91**, 3114 (2002).